

# Systematical study of $\Omega_c$ -like molecular states from interactions $\Xi_c^{(*,*)}\bar{K}^{(*)}$ and $\Xi^{(*)}D^{(*)}$

Jun-Tao Zhu, Shu-Yi Kong, Lin-Qing Song, and Jun He\*

School of Physics and Technology, Nanjing Normal University, Nanjing 210097, China

(Dated: May 25, 2022)

In this work, the  $\Omega_c$ -like molecular states are systematically investigated in a quasipotential Bethe-Salpeter equation approach. The relevant interactions  $\Xi_c^{(*,*)}\bar{K}^{(*)}$ ,  $\Xi^{(*)}D^{(*)}$ , and  $\Omega_c^{(*)}(\pi/\eta/\rho/\omega)$  are described by light meson exchanges with the help of the effective Lagrangians with SU(3), chiral, and heavy quark symmetries. The obtained potential kernels of considered interactions are inserted into the quasipotential Bethe-Salpeter equation, and coupled-channel calculations are performed to find possible molecular states and its couplings to the channels considered. The results suggest that an isoscalar state can be produced from the  $\Xi_c^*\bar{K}$  interaction with spin parity  $3/2^-$ , which can be related to state  $\Omega_c(3120)$ . And its isoscalar partner is predicted with a dominant decay in the  $\Omega_c^*\pi$  channel. The isoscalar and isovector states with  $1/2^-$  can be produced from the  $\Xi_c'\bar{K}$  interaction with a threshold close to the mass of the  $\Omega_c(3050)$  and  $\Omega_c(3065)$ . Their couplings to the  $\Xi_c\bar{K}$  channel are very weak, and the isovector one has strong coupling to  $\Omega_c\pi$ . High-precision measurement is helpful to confirm or search such molecular states. Experimental search of states with higher masses generated from interactions  $\Xi_c^{(*,*)}\bar{K}^{(*)}$  and  $\Xi^{(*)}D^{(*)}$  are also suggested by the current results.

## I. INTRODUCTION

In 2017, LHCb reported five narrow structures named  $\Omega_c(3000)$ ,  $\Omega_c(3050)$ ,  $\Omega_c(3065)$ ,  $\Omega_c(3090)$ , and  $\Omega_c(3120)$  in the  $\Xi_c^+K^-$  mass projection of the  $\Omega_b^- \rightarrow \Xi_c^+K^-\pi^-$  decays [1]. The Belle Collaboration confirmed the former four structures [2]. Many theoretical works were inspired by the observations to interpret their origins and internal structures, including calculations in the potential model [3–7], constituent quark model [8–21], QCD sum rule [22–24], lattice QCD [25], and other phenomenological approaches [26, 27]. One of the most popular interpretations is that the observed five peaks correspond to five excited  $\Omega_c$  baryons with spin parities  $J^P = 1/2^-, 1/2^-, 3/2^-, 3/2^-,$  and  $5/2^-$ , respectively. The  $\Omega_c(3120)$  and  $\Omega_c(3050)/\Omega_c(3065)$  are close to the  $\Xi_c^*\bar{K}$  and  $\Xi_c'\bar{K}$  thresholds, respectively. The molecular states picture was also applied to interpret some of five peaks as baryon-meson bound states [4–7, 19–21]. For example, in the chiral unitary approach, the theoretical masses and widths of a  $\Xi_c^*\bar{K}$  state with  $3/2^-$ , a  $\Xi D$  state with  $1/2^-$ , and a  $\Xi_c'\bar{K}$  state with  $1/2^-$  are in remarkable agreement with the experimentally observed  $\Omega_c(3120)$ ,  $\Omega_c(3090)$ , and  $\Omega_c(3050)$  [4]. In Ref. [7], a coupled-channel calculation indicates that either  $\Omega_c(3090)$  or  $\Omega_c(3120)$  is possibly to be related to isoscalar  $\Xi_c^*\bar{K}/\Omega_c\eta/\Omega_c^*\eta/\Xi_c\bar{K}^*/\Xi_c'\bar{K}^*/\Omega_c\omega$  state with spin parity  $3/2^-$ .

In 2021, the LHCb Collaboration updated its measurement about the  $\Omega_c$  structures [28]. The new analysis suggests that the spins of  $\Omega_c(3050)$  and  $\Omega_c(3065)$  tend not to be  $1/2$ . However,  $\Omega_c(3050)$  and  $\Omega_c(3065)$  are close to the  $\Xi_c'\bar{K}$  threshold. If we assign them as molecular states composed of the  $\Xi_c'\bar{K}$ , only spin parity  $1/2^-$  can be obtained in the  $S$  wave. Hence, the new result is inconsistent with the prediction of spin of the  $\Omega_c(3050)$  in previous theoretical works [4, 15, 22, 25]. In the Belle experiment [2] and new experiment at LHCb [28], the  $\Omega_c(3120)$  was not observed, though it is a good candidate of  $\Xi_c^*\bar{K}$  molecular state with

$3/2^-$ . In Ref. [28], it was suggested that the  $\Omega_c(3120)$  would be a state being either one of the  $2S$  doublet, or a  $\rho$ -mode  $P$ -wave excitation, which decays to  $\Xi_c^+K^-$  in the  $D$  wave, and then suppressed.

Up to now, the internal structures of these  $\Omega_c$ -like states are still not well understood. We should answer why the  $\Omega_c(3120)$  is so difficult to observe if it is a molecular state. If we accept the new LHCb results about the spin parities, the  $\Xi_c'\bar{K}$  molecular states should not be  $\Omega_c(3050)$  or  $\Omega_c(3065)$ . Where should we find them? In this work, we will investigate all  $\Omega_c$ -like baryon-meson interactions with flavor numbers  $C = 1$ ,  $S = -2$  under 3.6 GeV to find all possible molecular states from these interactions and discuss their relations to the experimentally observed structures. The couplings of these molecular states to the channels considered will also be studied through coupled-channel calculation. Besides, more molecular states will be predicted from these interactions, which are helpful to understand existing states and future experimental research.

Based on such consideration, we will consider interactions  $\Xi_c^{(*,*)}\bar{K}^{(*)}$ ,  $\Xi^{(*)}D^{(*)}$ , and  $\Omega_c^{(*)}(\eta/\omega/\pi/\rho)$  in the current work. As usual, only spin parities  $J^P$  of the interactions which can be produced in the  $S$ -wave will be included in the calculation. However, we would like to note that contributions from higher partial waves will also be included in our models for an interaction considered. All possible isospins and spin parities of all considered interactions are listed in Table I in order of mass threshold from large to small. Eighteen interactions are considered in the current work, and 48 channels will be involved after different isospins and spin parities are considered. In the calculation, these interactions can be divided into two categories:

- category I:  $\Xi^{(*)}D^{(*)}$ ;
- category II:  $\Xi_c^{(*,*)}\bar{K}^{(*)}$ ,  $\Omega_c^{(*)}(\pi/\eta/\rho/\omega)$ .

In the current work, the one-boson-exchange model will be adopted to describe the interactions. The interactions in category I are composed of a light baryon and a charmed meson, while the interactions in category II are composed of

\*Corresponding author: junhe@njnu.edu.cn

a charmed baryon and a light meson. The couplings between channels belonging to different categories intermediate only by exchanges of charmed mesons. It should be heavily suppressed and can be ignored compared with the couplings between the channels in the same category where light meson exchanges provide the dominant contribution. Besides, the  $\Omega_c^{(*)}(\pi/\eta/\rho/\omega)$  interaction in category II will be excluded in single-channel calculation in the current model due to the absence of possible meson exchange to provide attraction. However, these channels are not trivial in coupled-channel calculation.

TABLE I: The possible isospins and spin parities of all considered interactions. The thresholds are in the unit of MeV.

Channel	$\Omega_c^* \omega$	$\Xi^* D^*$	$\Omega_c^* \rho$	$\Xi_c^* \bar{K}^*$	$\Omega_c \omega$	$\Xi_c \bar{K}^*$
Threshold	3550.9	3541.8	3541.2	3540.2	3480.1	3470.7
$I = 0, J^P$	$(\frac{1}{2}, \frac{3}{2}, \frac{5}{2})^-$	$(\frac{1}{2}, \frac{3}{2}, \frac{5}{2})^-$	---	$(\frac{1}{2}, \frac{3}{2}, \frac{5}{2})^-$	$(\frac{1}{2}, \frac{3}{2})^-$	$(\frac{1}{2}, \frac{3}{2})^-$
$I = 1, J^P$	---	$(\frac{1}{2}, \frac{3}{2}, \frac{5}{2})^-$	$(\frac{1}{2}, \frac{3}{2}, \frac{5}{2})^-$	$(\frac{1}{2}, \frac{3}{2}, \frac{5}{2})^-$	---	$(\frac{1}{2}, \frac{3}{2})^-$
Channel	$\Omega_c \rho$	$\Xi^* D$	$\Xi_c \bar{K}^*$	$\Xi D^*$	$\Omega_c^* \eta$	$\Omega_c \eta$
Threshold	3470.5	3400.6	3363.3	3326.5	3315.8	3245.0
$I = 0, J^P$	---	$\frac{3}{2}^-$	$(\frac{1}{2}, \frac{3}{2})^-$	$(\frac{1}{2}, \frac{3}{2})^-$	$\frac{3}{2}^-$	$\frac{1}{2}^-$
$I = 1, J^P$	$(\frac{1}{2}, \frac{3}{2})^-$	$\frac{3}{2}^-$	$(\frac{1}{2}, \frac{3}{2})^-$	$(\frac{1}{2}, \frac{3}{2})^-$	---	---
Channel	$\Xi D$	$\Xi_c^* \bar{K}$	$\Xi_c' \bar{K}$	$\Xi_c \bar{K}$	$\Omega_c^* \pi$	$\Omega_c \pi$
Threshold	3185.3	3142.0	3072.5	2965.1	2903.1	2832.4
$I = 0, J^P$	$\frac{1}{2}^-$	$\frac{3}{2}^-$	$\frac{1}{2}^-$	$\frac{1}{2}^-$	---	---
$I = 1, J^P$	$\frac{1}{2}^-$	$\frac{3}{2}^-$	$\frac{1}{2}^-$	$\frac{1}{2}^-$	$\frac{3}{2}^-$	$\frac{1}{2}^-$

This article is organized as follows. In the next section, the effective Lagrangians will be provided to construct potentials of considered interactions  $\Xi^{(*)}D^{(*)}$ ,  $\Xi_c^{(*)}K^{(*)}$ , and  $\Omega_c^{(*)}(\pi/\eta/\rho/\omega)$  in the one-boson-exchange model. The quasipotential Bethe-Salpeter equation approach adopted in the current work will be also introduced briefly in that section. The results with single-channel calculation will be presented in section III. And couplings between different interactions will be specifically described and discussed in section IV. Finally, the article ends with summary and discussion in section V.

## II. THEORETICAL FRAME

All systems considered in the current work are composed of a charmed and a light hadron. The Lagrangians for the charmed and light hadrons will be presented in the following.

### A. Lagrangians for charmed hadrons

The Lagrangians for the vertex of charmed hadrons and light mesons have been constructed under the heavy quark limit and chiral symmetry in the literature [29–32]. The couplings of heavy-light charmed mesons  $\mathcal{P}^{(*)} =$

$(D^{(*)0}, D^{(*)+}, D_s^{(*)+})$  and light exchange mesons can be depicted as

$$\begin{aligned}
\mathcal{L}_{\mathcal{P}^* \mathcal{P}^* \mathbb{P}} &= i \frac{2g \sqrt{m_{\mathcal{P}^*} m_{\mathbb{P}}}}{f_{\pi}} (-\mathcal{P}_{a\lambda}^{*\dagger} \mathcal{P}_b + \mathcal{P}_a^{\dagger} \mathcal{P}_{b\lambda}^*) \partial^{\lambda} \mathbb{P}_{ab}, \\
\mathcal{L}_{\mathcal{P}^* \mathcal{P}^* \mathbb{P}} &= -\frac{g}{f_{\pi}} \epsilon_{\alpha\mu\nu\lambda} \mathcal{P}_a^{*\mu\dagger} \overleftrightarrow{\partial}^{\alpha} \mathcal{P}_b^* \partial^{\nu} \mathbb{P}_{ba}, \\
\mathcal{L}_{\mathcal{P}^* \mathcal{P}^* \mathbb{V}} &= \sqrt{2} \lambda g_V \epsilon_{\lambda\alpha\beta\mu} (-\mathcal{P}_a^{*\mu\dagger} \overleftrightarrow{\partial}^{\lambda} \mathcal{P}_b + \mathcal{P}_a^{\dagger} \overleftrightarrow{\partial}^{\lambda} \mathcal{P}_b^*) (\partial^{\alpha} \mathbb{V}^{\beta})_{ab}, \\
\mathcal{L}_{\mathcal{P}^* \mathcal{P}^* \mathbb{V}} &= -i \frac{\beta g_V}{\sqrt{2}} \mathcal{P}_a^{\dagger} \overleftrightarrow{\partial}_{\mu} \mathcal{P}_b^* \mathbb{V}_{ab}^{\mu}, \\
\mathcal{L}_{\mathcal{P}^* \mathcal{P}^* \mathbb{V}} &= i \frac{\beta g_V}{\sqrt{2}} \mathcal{P}_a^{*\dagger} \overleftrightarrow{\partial}_{\mu} \mathcal{P}_b^* \mathbb{V}_{ab}^{\mu} \\
&\quad - i 2 \sqrt{2} \lambda g_V m_{\mathcal{P}^*} \mathcal{P}_a^{*\dagger} \mathcal{P}_b^* (\partial_{\mu} \mathbb{V}_{\nu} - \partial_{\nu} \mathbb{V}_{\mu})_{ab}, \\
\mathcal{L}_{\mathcal{P}^* \mathcal{P}^* \sigma} &= -2 g_s m_{\mathcal{P}^*} \mathcal{P}_a^{\dagger} \mathcal{P}_a \sigma, \\
\mathcal{L}_{\mathcal{P}^* \mathcal{P}^* \sigma} &= 2 g_s m_{\mathcal{P}^*} \mathcal{P}_a^{*\dagger} \mathcal{P}_a^* \sigma,
\end{aligned} \tag{1}$$

where  $m_{\mathcal{P}^{(*)}}$  is the mass of  $\mathcal{P}^{(*)}$  and  $\overleftrightarrow{\partial} = \overrightarrow{\partial} - \overleftarrow{\partial}$ . The  $\mathcal{P}$  and  $\mathcal{P}^*$  satisfy the normalization relations  $\langle 0 | \mathcal{P} | \bar{Q} q(0^-) \rangle = \sqrt{m_{\mathcal{P}}}$  and  $\langle 0 | \mathcal{P}_{\mu}^* | \bar{Q} q(1^-) \rangle = \epsilon_{\mu} \sqrt{m_{\mathcal{P}^*}}$ . The  $\mathbb{P}$  and  $\mathbb{V}$  are the pseudoscalar and vector matrices,

$$\mathbb{P} = \begin{pmatrix} \frac{\sqrt{3}\pi^0 + \eta}{\sqrt{6}} & \pi^+ & K^+ \\ \pi^- & -\frac{\sqrt{3}\pi^0 + \eta}{\sqrt{6}} & K^0 \\ K^- & \bar{K}^0 & \frac{-2\eta}{\sqrt{6}} \end{pmatrix}, \quad \mathbb{V} = \begin{pmatrix} \frac{\rho^0 + \omega}{\sqrt{2}} & \rho^+ & K^{*+} \\ \rho^- & \frac{-\rho^0 + \omega}{\sqrt{2}} & K^{*0} \\ K^{*-} & \bar{K}^{*0} & \phi \end{pmatrix}. \tag{2}$$

The Lagrangians for the couplings between charmed baryon and light exchanged meson can also be constructed under the heavy quark limit and chiral symmetry, and the explicit forms of these Lagrangians can be written as [33]

$$\begin{aligned}
\mathcal{L}_{BB\mathbb{P}} &= -\frac{3g_1}{4f_{\pi} \sqrt{m_{\bar{B}} m_B}} \epsilon^{\mu\nu\lambda\kappa} \partial^{\nu} \mathbb{P} \sum_{i=0,1} \bar{B}_i^{\mu} \overleftrightarrow{\partial}_{\kappa} B_{j\lambda}, \\
\mathcal{L}_{BB\mathbb{V}} &= -i \frac{\beta_S g_V}{2 \sqrt{2} m_{\bar{B}} m_B} \mathbb{V}^{\nu} \sum_{i=0,1} \bar{B}_i^{\mu} \overleftrightarrow{\partial}_{\nu} B_{j\mu} \\
&\quad - i \frac{\lambda_S g_V}{\sqrt{2}} (\partial_{\mu} \mathbb{V}_{\nu} - \partial_{\nu} \mathbb{V}_{\mu}) \sum_{i=0,1} \bar{B}_i^{\mu} B_j^{\nu}, \\
\mathcal{L}_{BB\sigma} &= \ell_S \sigma \sum_{i=0,1} \bar{B}_i^{\mu} B_{j\mu}, \\
\mathcal{L}_{B_3 B_3 \mathbb{V}} &= -i \frac{g_V \beta_B}{2 \sqrt{2} m_{\bar{B}_3} m_{B_3}} \mathbb{V}^{\mu} \bar{B}_3^{\mu} \overleftrightarrow{\partial}_{\mu} B_3, \\
\mathcal{L}_{B_3 B_3 \sigma} &= \ell_B \sigma \bar{B}_3 B_3, \\
\mathcal{L}_{BB_3 \mathbb{P}} &= -i \frac{g_4}{f_{\pi}} \sum_i \bar{B}_i^{\mu} \partial_{\mu} \mathbb{P} B_3 + \text{H.c.}, \\
\mathcal{L}_{BB_3 \mathbb{V}} &= \frac{g_V \lambda_I}{\sqrt{2} m_{\bar{B}} m_{B_3}} \epsilon^{\mu\nu\lambda\kappa} \partial_{\lambda} \mathbb{V}_{\kappa} \sum_i \bar{B}_{i\nu} \overleftrightarrow{\partial}_{\mu} B_3 + \text{H.c.}
\end{aligned} \tag{3}$$

where  $S_{ab}^{\mu}$  read

$$B_{0\mu}^{ab} = -\sqrt{\frac{1}{3}} (\gamma_{\mu} + v_{\mu}) \gamma^5 B^{ab}, \quad B_{1\mu}^{ab} = B_{\mu}^{*ab},$$

$$\bar{B}_{0\mu}^{ab} = \sqrt{\frac{1}{3}} \bar{B}^{ab} \gamma^5 (\gamma_\mu + \nu_\mu), \quad \bar{B}_{1\mu}^{ab} = \bar{B}_\mu^{*ab}, \quad (4)$$

with the charmed baryon matrices being defined as

$$B_{\bar{3}} = \begin{pmatrix} 0 & \Lambda_c^+ & \Xi_c^+ \\ -\Lambda_c^+ & 0 & \Xi_c^0 \\ -\Xi_c^+ & -\Xi_c^0 & 0 \end{pmatrix}, \quad B = \begin{pmatrix} \Sigma_c^{++} & \frac{1}{\sqrt{2}} \Sigma_c^+ & \frac{1}{\sqrt{2}} \Xi_c^{'+} \\ \frac{1}{\sqrt{2}} \Sigma_c^+ & \Sigma_c^0 & \frac{1}{\sqrt{2}} \Xi_c'^0 \\ \frac{1}{\sqrt{2}} \Xi_c^{'+} & \frac{1}{\sqrt{2}} \Xi_c'^0 & \Omega_c^0 \end{pmatrix}. \quad (5)$$

$$B^* = \begin{pmatrix} \Sigma_c^{*++} & \frac{1}{\sqrt{2}} \Sigma_c^{*+} & \frac{1}{\sqrt{2}} \Xi_c^{*'+} \\ \frac{1}{\sqrt{2}} \Sigma_c^{*+} & \Sigma_c^{*0} & \frac{1}{\sqrt{2}} \Xi_c^{*0} \\ \frac{1}{\sqrt{2}} \Xi_c^{*'+} & \frac{1}{\sqrt{2}} \Xi_c^{*0} & \Omega_c^{*0} \end{pmatrix}.$$

The masses of particles involved in the calculation are chosen as suggested central values in the Review of Particle Physics (PDG) [34]. The mass of the broad scalar  $\sigma$  meson is chosen as 500 MeV. The coupling constants involved are listed in Table II.

TABLE II: The coupling constants adopted in the calculation, which are cited from the literature [33, 35–37]. The  $\lambda$ ,  $\lambda_{S,I}$ , and  $f_\pi$  are in the unit of  $\text{GeV}^{-1}$ . Others are in units of 1.

$\beta$	$g$	$g_V$	$\lambda$	$g_S$	$f_\pi$		
0.9	0.59	5.9	0.56	0.76	0.132		
$\beta_S$	$\ell_S$	$g_1$	$\lambda_S$	$\beta_B$	$\ell_B$	$g_4$	$\lambda_I$
-1.74	6.2	-0.94	-3.31	$-\beta_S/2$	$-\ell_S/2$	$3g_1/(2\sqrt{2})$	$-\lambda_S/\sqrt{8}$

## B. Lagrangians for light hadrons

In the following we will present the Lagrangians for the vertex of the constituent light hadrons  $\bar{K}^{(*)}$  or  $\Xi^{(*)}$  and the exchanged light hadrons  $m$ . The vertices  $\bar{K}^{(*)} \bar{K}^{(*)} m$  and  $\Xi^{(*)} \Xi^{(*)} m$  can be related to vertices  $\pi\pi m$ ,  $\rho\rho m$ ,  $\rho\omega m$ ,  $NNm$ ,  $\Delta\Delta m$ , and  $N\Delta$  under SU(3) flavor symmetry [38–40]. First, the Lagrangians for  $\bar{K}^{(*)} \bar{K}^{(*)} m$  are shown as

$$\begin{aligned} \mathcal{L}_{\bar{K}\bar{K}V} &= ig_{\bar{K}\bar{K}V} \bar{K}^\dagger V^\mu \overleftrightarrow{\partial}_\mu \bar{K}, \\ \mathcal{L}_{\bar{K}\bar{K}\sigma} &= -g_{\bar{K}\bar{K}\sigma} \bar{K}^\dagger \sigma \bar{K}, \\ \mathcal{L}_{\bar{K}^* \bar{K}^* P} &= g_{\bar{K}^* \bar{K}^* P} \epsilon^{\mu\nu\alpha\beta} \partial_\mu \bar{K}_\nu^{*\dagger} \partial_\alpha P \bar{K}_\beta^*, \\ \mathcal{L}_{\bar{K}^* \bar{K}^* V} &= -i \frac{g_{\bar{K}^* \bar{K}^* V}}{2} (\bar{K}^{*\mu\dagger} V_{\mu\nu} \bar{K}^{*\nu} + \bar{K}_{\mu\nu}^{*\dagger} V^\mu \bar{K}^{*\nu} + \bar{K}^{*\mu\dagger} V^\nu \bar{K}_{\nu\mu}^*), \\ \mathcal{L}_{\bar{K}^* \bar{K}^* \sigma} &= g_{\bar{K}^* \bar{K}^* \sigma} \bar{K}^{*\mu\dagger} \sigma \bar{K}^{*\mu}, \\ \mathcal{L}_{\bar{K} \bar{K}^* P} &= ig_{\bar{K} \bar{K}^* P} \bar{K}_\mu^{*\dagger} P \partial_\mu \bar{K} + h.c., \\ \mathcal{L}_{\bar{K} \bar{K}^* V} &= g_{\bar{K} \bar{K}^* V} \epsilon^{\mu\nu\alpha\beta} \partial_\mu \bar{K}_\nu^{*\dagger} \partial_\alpha P \bar{K}_\beta, \end{aligned} \quad (6)$$

where the  $P$  and  $V_\mu$  in the Lagrangians stand for the pseudoscalar meson ( $\vec{\tau} \cdot \vec{\pi}$  or  $\eta$ ) and vector meson ( $\vec{\tau} \cdot \vec{\rho}_\mu$ ,  $\omega_\mu$ , or  $\phi_\mu$ ), respectively;  $V_{\mu\nu} = \partial_\mu V_\nu - \partial_\nu V_\mu$ . The coupling constants can be obtained by the SU(3) relation and are listed in Table III.

The Lagrangians for vertices of light baryon coupling with a light exchanged mesons  $\Xi^{(*)} \Xi^{(*)} m$  are written as

$$\mathcal{L}_{\Xi\Xi P} = -\frac{g_{\Xi\Xi P}}{m_P} \bar{\Xi} \gamma^5 \gamma^\mu \partial_\mu P \Xi,$$

TABLE III: The coupling constants determined with SU(3) symmetry. The values are in the unit of GeV. The three basic constants are chosen as  $g_{PPV} = 3.02$ ,  $g_{VVP} = 5.6$  and  $g_{VVV} = 3.25$  [39].

Coupl.	SU(3) relation	Values	Coupl.	SU(3) relation	Values
$g_{\bar{K}^* \bar{K}^* \pi}$	$g_{VVP}$	5.6	$g_{\bar{K}^* \bar{K}^* \eta}$	$-\sqrt{3}g_{VVP}$	-9.7
$g_{\bar{K}^* \bar{K}^* \rho}$	$g_{VVV}$	3.25	$g_{\bar{K}^* \bar{K}^* \omega}$	$-g_{VVV}$	-3.25
$g_{\bar{K}^* \bar{K}^* \phi}$	$-\sqrt{2}g_{VVV}$	-4.6	$g_{\bar{K}^* \bar{K}^* \sigma}$	--	3.65
$g_{\bar{K} \bar{K} \rho}$	$g_{PPV}$	3.02	$g_{\bar{K} \bar{K} \omega}$	$-g_{PPV}$	-3.02
$g_{\bar{K} \bar{K} \phi}$	$-\sqrt{2}g_{PPV}$	-4.27	$g_{\bar{K} \bar{K} \sigma}$	--	3.65
$g_{\bar{K} \pi \bar{K}^*}$	$-g_{PPV}$	-3.02	$g_{\bar{K} \eta \bar{K}^*}$	$\sqrt{3}g_{PPV}$	5.23
$g_{\bar{K}^* \rho \bar{K}}$	$g_{VVP}$	5.6	$g_{\bar{K}^* \omega \bar{K}}$	$-g_{VVP}$	-5.6
$g_{\bar{K}^* \phi \bar{K}}$	$-\sqrt{2}g_{VVP}$	-7.92			

$$\mathcal{L}_{\Xi\Xi V} = -\bar{\Xi} [g_{\Xi\Xi V} \gamma^\mu - \frac{f_{\Xi\Xi V}}{2m_\Xi} \sigma^{\mu\nu} \partial_\nu] V_\mu \Xi,$$

$$\mathcal{L}_{\Xi\Xi\sigma} = -g_{\Xi\Xi\sigma} \bar{\Xi} \sigma \Xi,$$

$$\mathcal{L}_{\Xi^* \Xi^* P} = -\frac{g_{\Xi^* \Xi^* P}}{m_P} \bar{\Xi}^{*\alpha} \gamma^5 \gamma^\mu \partial_\mu P \Xi_\alpha^*,$$

$$\mathcal{L}_{\Xi^* \Xi^* V} = -\bar{\Xi}^{*\alpha} [g_{\Xi^* \Xi^* V} \gamma^\mu - \frac{f_{\Xi^* \Xi^* V}}{2m_{\Xi^*}} \sigma^{\mu\nu} \partial_\nu] V_\mu \Xi_\alpha^*,$$

$$\mathcal{L}_{\Xi^* \Xi^* \sigma} = g_{\Xi^* \Xi^* \sigma} \bar{\Xi}^{*\mu} \sigma \Xi_\mu^*,$$

$$\mathcal{L}_{\Xi\Xi^* P} = \frac{g_{\Xi\Xi^* P}}{m_P} \bar{\Xi}^{*\mu} \partial_\mu P \Xi + h.c.,$$

$$\mathcal{L}_{\Xi\Xi^* V} = -i \frac{g_{\Xi\Xi^* V}}{m_V} \bar{\Xi}^{*\mu} \gamma^5 \gamma^\nu V_{\mu\nu} \Xi + h.c.. \quad (7)$$

With the help of the SU(3) symmetry, the values of the coupling constants are given in Table IV. Here, we choose  $\alpha_{BBV} = 1.15$  as in Ref. [39] based on the  $NN\omega$  coupling constant given in Refs. [41, 42] differing from the standard value  $\alpha_{BBV} = 1$ , which introduces a small SU(3) symmetry breaking in all vector-meson couplings. Furthermore, we adopt  $f_{NN\omega} = 0$  with  $f_{BBV} = g_{BBV} \kappa_V$ ,  $f_{DDV} = g_{DDV} \kappa_V$ , and  $\kappa_\rho = 6.1$ .

TABLE IV: The values of coupling constants and SU(3) relations. The values are in the unit of GeV. The basic constants  $g_{BBP} = 0.989$ ,  $g_{BBV} = 3.25$ ,  $\alpha_{BBP} = 0.4$ ,  $\alpha_{BBV} = 1.15$  and  $g_{BB\sigma} = 6.59$ ;  $g_{DDP} = 13.79$ ,  $g_{DDV} = 59.41$ ,  $g_{BDP} = 9.48$ , and  $g_{BDP} = 71.69$  [39, 40].

Coupl.	SU(3) relation	Values	Coupl.	SU(3) relation	Values
$g_{\Xi\Xi\pi}$	$(2\alpha - 1)g_{BBP}$	-0.20	$g_{\Xi\Xi\eta}$	$-\frac{\sqrt{3}(1+2\alpha)}{3}g_{BBP}$	-1.03
$g_{\Xi\Xi\rho}$	$(2\alpha - 1)g_{BBV}$	4.23	$g_{\Xi\Xi\omega}$	$(2\alpha - 1)g_{BBV}$	4.23
$g_{\Xi\Xi\sigma}$	$g_{BB\sigma}$	6.59	$g_{\Xi^* \Xi^* \sigma}$	$g_{BB\sigma}$	6.59
$g_{\Xi^* \Xi^* \pi}$	$\frac{1}{4\sqrt{15}}g_{DDP}$	0.89	$g_{\Xi^* \Xi^* \eta}$	$-\frac{1}{4\sqrt{15}}g_{DDP}$	-1.54
$g_{\Xi^* \Xi^* \rho}$	$\frac{1}{4\sqrt{15}}g_{DDV}$	3.84	$g_{\Xi^* \Xi^* \omega}$	$\frac{1}{4\sqrt{15}}g_{DDV}$	3.84
$g_{\Xi\Xi^* \pi}$	$\frac{1}{2\sqrt{30}}g_{BDP}$	0.87	$g_{\Xi\Xi^* \eta}$	$-\frac{1}{2\sqrt{10}}g_{BDP}$	-1.50
$g_{\Xi\Xi^* \rho}$	$\frac{1}{2\sqrt{30}}g_{BDV}$	6.54	$g_{\Xi\Xi^* \omega}$	$-\frac{1}{2\sqrt{30}}g_{BDV}$	-6.54
$f_{\Xi\Xi\rho}$	$\frac{1}{2}(f_{NN\omega} - f_{NN\rho})$	-9.9	$f_{\Xi\Xi\omega}$	$\frac{1}{2}(f_{NN\omega} - f_{NN\rho})$	-9.9
$f_{\Xi^* \Xi^* \rho}$	$\frac{1}{4\sqrt{15}}f_{\Delta\Delta\rho}$	29.4	$f_{\Xi^* \Xi^* \omega}$	$\frac{1}{4\sqrt{15}}f_{\Delta\Delta\rho}$	29.4

### C. Potential kernels

The isospin wave functions for the systems considered in the current work can be written as,

$$\begin{aligned}
|\Xi^{(*)}D^{(*)}, I=0\rangle &= -\frac{1}{\sqrt{2}}|\Xi^{(*)0}D^{(*)0} + \Xi^-D^+\rangle, \\
|\Xi^{(*)}D^{(*)}, I=1\rangle &= -\frac{1}{\sqrt{2}}|\Xi^{(*)0}D^{(*)0} - \Xi^*D^+\rangle, \\
|\Xi_c^{(*)'}\bar{K}^{(*)}, I=0\rangle &= -\frac{1}{\sqrt{2}}|\Xi_c^{(*)'+}K^{(*)-} + \Xi_c^{(*)0}\bar{K}^{(*)0}\rangle, \\
|\Xi_c^{(*)'}\bar{K}^{(*)}, I=1\rangle &= -\frac{1}{\sqrt{2}}|\Xi_c^{(*)'+}K^{(*)-} - \Xi_c^{(*)0}\bar{K}^{(*)0}\rangle, \\
|\Omega_c^{(*)}\omega(\eta), I=0\rangle &= |\Omega_c^{(*)0}\omega(\eta)\rangle, \\
|\Omega_c^{(*)}\rho(\pi), I=1\rangle &= |\Omega_c^{(*)0}\rho^0(\pi^0)\rangle. \tag{8}
\end{aligned}$$

Here, the isospin multiplets are defined as

$$\begin{aligned}
D^{(*)} &= \begin{pmatrix} D^{(*)+} \\ -D^{(*)0} \end{pmatrix}, \quad \Xi^{(*)} = \begin{pmatrix} \Xi^{(*)0} \\ \Xi^{(*)-} \end{pmatrix}; \\
\bar{K}^{(*)} &= \begin{pmatrix} \bar{K}^{(*)0} \\ -K^{(*)-} \end{pmatrix}, \quad \Xi_c^{(*)} = \begin{pmatrix} \Xi_c^{(*)+} \\ \Xi_c^{(*)0} \end{pmatrix}, \quad \Xi_c^{(*)'} = \begin{pmatrix} \Xi_c^{(*)'+} \\ \Xi_c^{(*)'0} \end{pmatrix}. \tag{9}
\end{aligned}$$

With the vertices obtained from the above Lagrangians, the potential kernels of coupled-channel interactions can be constructed easily with the help of the standard Feynman rules. In this work, following the method in Refs. [43–45], we input vertices  $\Gamma$  and propagators  $P$  into the code directly. The potential can be written as

$$\mathcal{V}_{\mathbb{P},\sigma} = I_{\mathbb{P},\sigma}\Gamma_1\Gamma_2P_{\mathbb{P},\sigma}f(q^2), \quad \mathcal{V}_{\mathbb{V}} = I_{\mathbb{V}}\Gamma_{1\mu}\Gamma_{2\nu}P_{\mathbb{V}}^{\mu\nu}f(q^2). \tag{10}$$

The propagators are defined as usual as

$$P_{\mathbb{P},\sigma} = \frac{i}{q^2 - m_{\mathbb{P},\sigma}^2}, \quad P_{\mathbb{V}}^{\mu\nu} = i \frac{-g^{\mu\nu} + q^\mu q^\nu / m_{\mathbb{V}}^2}{q^2 - m_{\mathbb{V}}^2}, \tag{11}$$

The form factor  $f(q^2)$  is adopted to compensate the off-shell effect of exchanged meson as  $f(q^2) = e^{-(m_e^2 - q^2)^2 / \Lambda_e^4}$  with  $m_e$  and  $q$  being the mass and momentum of the exchanged meson. The flavor factor  $I_{ex}$  can be obtained with the wave functions and Lagrangians as listed in Table V.

The potential kernel obtained in Eq. (10) can be projected into fixed spin-parity by partial-wave decomposition as

$$\begin{aligned}
\mathcal{V}_{\lambda'\lambda}^{Jp}(\mathbf{p}', \mathbf{p}) &= 2\pi \int d\cos\theta [d_{\lambda'\lambda}^J(\theta)\mathcal{V}_{\lambda'\lambda}(\mathbf{p}', \mathbf{p}) \\
&\quad + \eta d_{-\lambda'\lambda}^J(\theta)\mathcal{V}_{\lambda'\lambda}(\mathbf{p}', \mathbf{p})], \tag{12}
\end{aligned}$$

where  $\eta = PP_1P_2(-1)^{J-J_1-J_2}$  with  $P$  and  $J$  being parity and spin for the system. The initial and final relative momenta are chosen as  $\mathbf{p} = (0, 0, p)$  and  $\mathbf{p}' = (p' \sin\theta, 0, p' \cos\theta)$ . The  $d_{\lambda'\lambda}^J(\theta)$  is the Wigner  $d$  matrix.

TABLE V: The flavor factor  $I_{ex}$  for a system with certain isospin and meson exchange. The vertices for three pseudoscalar mesons should be forbidden.

<hr/>							
Transition	$\Xi^{(*)}D^{(*)} \rightarrow \Xi^{(*)}D^{(*)}$						
$I_{ex}$	$I_\pi$	$I_\eta$	$I_\rho$	$I_\omega$	$I_\phi$	$I_\sigma$	
$I=0$	$3/\sqrt{2}$	$1/\sqrt{6}$	$3/\sqrt{2}$	$1/\sqrt{2}$	---	1	
$I=1$	$-1/\sqrt{2}$	$1/\sqrt{6}$	$-1/\sqrt{2}$	$1/\sqrt{2}$	---	1	
Transition	$\Xi_c^{(*)'}\bar{K}^{(*)} \rightarrow \Xi_c^{(*)'}\bar{K}^{(*)}$						
$I_{ex}$	$I_\pi$	$I_\eta$	$I_\rho$	$I_\omega$	$I_\phi$	$I_\sigma$	
$I=0$	$-3/2\sqrt{2}$	$-1/2\sqrt{6}$	$-3/2\sqrt{2}$	$1/2\sqrt{2}$	$1/2$	1	
$I=1$	$1/2\sqrt{2}$	$-1/2\sqrt{6}$	$1/2\sqrt{2}$	$1/2\sqrt{2}$	$1/2$	1	
Transition	$\Xi_c\bar{K}^{(*)} \rightarrow \Xi_c\bar{K}^{(*)}$						
$I_{ex}$	$I_\pi$	$I_\eta$	$I_\rho$	$I_\omega$	$I_\phi$	$I_\sigma$	
$I=0$	---	---	$-3/\sqrt{2}$	$1/\sqrt{2}$	1	2	
$I=1$	---	---	$1/\sqrt{2}$	$1/\sqrt{2}$	1	2	
Transition	$\Xi_c^{(*)'}\bar{K}^{(*)} \rightarrow \Xi_c\bar{K}^{(*)}$						
$I_{ex}$	$I_\pi$	$I_\eta$	$I_\rho$	$I_\omega$	$I_\phi$	$I_\sigma$	
$I=0$	$-3/2$	$\sqrt{3}/2$	$-3/2$	$1/2$	1	---	
$I=1$	$1/2$	$\sqrt{3}/2$	$1/2$	$1/2$	1	---	
Transition	$\Omega_c^{(*)}\eta/\omega \rightarrow \Xi_c^{(*)'}/\bar{K}^{(*)}$						
$I_{ex}$	$I_K$	$I_{K^*}$					
$I=0$	-1	-1					
Transition	$\Omega_c^{(*)}\pi/\rho \rightarrow \Xi_c^{(*)'}\bar{K}^{(*)}$						
$I_{ex}$	$I_K$	$I_{K^*}$					
$I=1$	1	1					
Transition	$\Omega_c^{(*)}\eta/\omega \rightarrow \Xi_c\bar{K}^{(*)}$						
$I_{ex}$	$I_K$	$I_{K^*}$					
$I=0$	$-\sqrt{2}$	$-\sqrt{2}$					
Transition	$\Omega_c^{(*)}\pi/\rho \rightarrow \Xi_c\bar{K}^{(*)}$						
$I_{ex}$	$I_K$	$I_{K^*}$					
$I=1$	$\sqrt{2}$	$\sqrt{2}$					
<hr/>							

To obtain the scattering amplitude, such partial-wave potential kernel can be inserted into the partial-wave quasipotential Bethe-Salpeter equation as [46–50]

$$\begin{aligned}
i\mathcal{M}_{\lambda'\lambda}^{Jp}(\mathbf{p}', \mathbf{p}) &= i\mathcal{V}_{\lambda'\lambda}^{Jp}(\mathbf{p}', \mathbf{p}) + \sum_{\lambda'' \geq 0} \int \frac{\mathbf{p}''^2 d\mathbf{p}''}{(2\pi)^3} \\
&\quad \cdot i\mathcal{V}_{\lambda'\lambda''}^{Jp}(\mathbf{p}', \mathbf{p}'')G_0(\mathbf{p}'')i\mathcal{M}_{\lambda''\lambda}^{Jp}(\mathbf{p}'', \mathbf{p}), \tag{13}
\end{aligned}$$

The reduced propagator  $G_0(\mathbf{p}'')$  under quasipotential approximation has a form of  $G_0(\mathbf{p}'') = \delta^+(p_h''^2 - m_h^2)/(p_l''^2 - m_l^2)$  with  $p_{h,l}''$  and  $m_{h,l}$  being the momenta and masses of heavy or light constituent particles. Since in the current approach, one of the constituent particles is put on shell while another is put off shell, an exponential regularization is also introduced as  $G_0(\mathbf{p}'') \rightarrow G_0(\mathbf{p}'') [e^{-(p_l''^2 - m_l^2)^2 / \Lambda_r^4}]^2$  with  $\Lambda_r$  being a cutoff [47]. To make it more in line with the values of different exchange mesons, a parameterization on the cutoff is performed as  $\Lambda_e = \Lambda_r = m_e + \alpha 0.22 \text{ GeV}$  with  $m_e$  being the mass of the exchange meson.

The partial-wave Bethe-Salpeter equation can be transformed into a matrix equation as  $M = V + VG_0M$  by Gauss discretizing, with which the scattering amplitude can be obtained as  $M(z) = V(z)/(1 - V(z)G_0(z))$ . The molecular state can be found at the pole of scattering amplitude in the complex energy plane when its denominator  $|1 - V(z)G_0(z)| = 0$ . The real and imaginary parts of the pole position  $z = W + i\Gamma/2$  are energy and half of the decay width, respectively.

### III. RESULTS WITH SINGLE-CHANNEL CALCULATION

Because of the complexity of the coupled-channel results, the results with single-channel calculation will be first presented in this section, which can provide an overall picture of the molecular states produced from the interactions considered.

#### A. Category I: Interaction $\Xi^{(*)}D^{(*)}$

In Fig. 1, the binding energies of all bound states produced from interaction  $\Xi^{(*)}D^{(*)}$  are presented with the variation of the  $\alpha$ , which is the only variable parameter in the current model, and absorbs the model uncertainties. Empirically, its value is chosen in a reasonable range from 0 to 5. Since the molecular state is defined as a shallow bound state, in the current work, we only keep the results with binding energy lower than 45 MeV or smaller.

The single-channel calculation suggests that only the isoscalar bound state can be produced from the interactions. No isovector state is found in the considered range of the parameter. Three isoscalar  $\Xi^*D^*$  states appear at almost the same value of  $\alpha$  about 1 with spin parities  $J^P = 1/2^-, 3/2^-,$  and  $5/2^-$ , which are all possible spin parities in the  $S$ -wave. The binding energies of all three states gradually increase with the increase of the  $\alpha$ . When  $\alpha$  increases to 4 or larger, the repulsion from  $\pi$  exchange increases faster than the attraction, which makes the state with  $1/2^-$  shallower.

Different from the  $\Xi^*D^*$  interaction, only one molecular state can be produced from the  $\Xi^*D$  interaction with spin parity  $3/2^-$ . For two lower interactions  $\Xi D^*$  and  $\Xi D$ , no bound state is found near their thresholds for all quantum numbers considered in the current work as listed in Table I.

#### B. Category II: Interaction $\Xi_c^{(*)}\bar{K}^{(*)}$

Six interactions in category II,  $\Xi_c^*\bar{K}^*$ ,  $\Xi_c'\bar{K}^*$ ,  $\Xi_c\bar{K}^*$ ,  $\Xi_c^*\bar{K}$ ,  $\Xi_c'\bar{K}$ , and  $\Xi_c\bar{K}$ , involve in the single-channel calculation. We first present the binding energies of isoscalar states with  $I = 0$  from these interactions in Fig. 2.

The  $\Xi_c^*\bar{K}^*$  interaction is found attractive and produces three isoscalar bound states with spin parities  $1/2^-, 3/2^-$ , and  $5/2^-$ , which all appear at a value of  $\alpha$  of about 1. Their binding energies increase with the increase of the parameter  $\alpha$ . The binding energies of states with larger spin increase more rapidly. Two bound states are produced from the  $\Xi_c'\bar{K}^*$

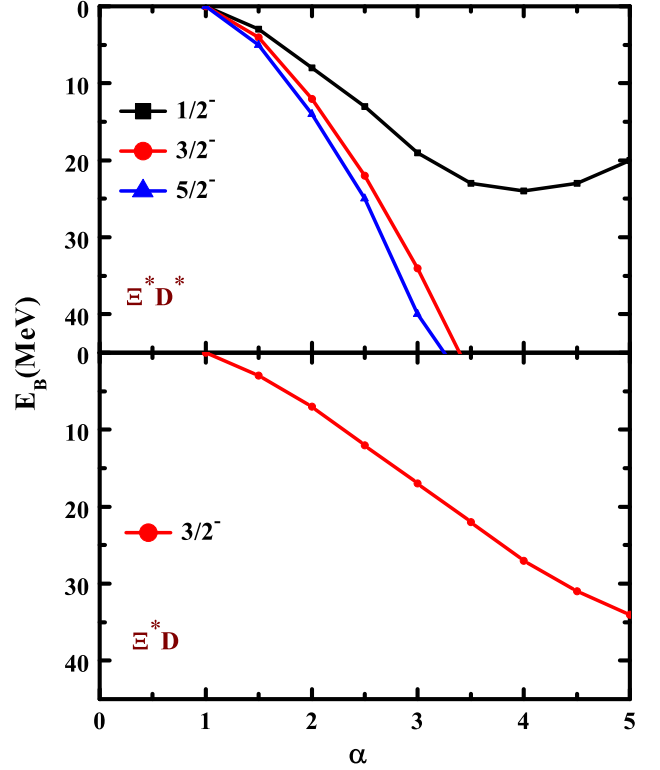


FIG. 1: The binding energies for the isoscalar bound states from interaction  $\Xi^{(*)}D^{(*)}$  with variation of  $\alpha$  with single-channel calculation. The upper and lower panels are for interactions  $\Xi^*D^*$  and  $\Xi^*D$ , respectively.

interaction with  $1/2^-$  and  $3/2^-$ . Large binding energy is also found for large spin parity  $3/2^-$ . The bound states from interaction  $\Xi_c\bar{K}^*$  with  $1/2^-$  and  $3/2^-$  are almost degenerate. It is from small differences of the vector exchange for different spin parities and the absence of pseudoscalar exchange as shown in Table V. A very large  $\alpha$  value is required to provide the obvious difference in binding energy.

As shown in the panels in the right of Fig. 2, only one bound state is produced for each of the interactions,  $\Xi_c^*\bar{K}$ ,  $\Xi_c'\bar{K}$ , or  $\Xi_c\bar{K}$ , and all of them appear at a value of  $\alpha$  of about 0.5. The curve of the binding energy of  $\Xi_c^*\bar{K}$  state with  $3/2^-$  is compared with the experimental mass of the  $\Omega_c(3120)$  as a horizontal line. The cross can be found at an  $\alpha$  value of about 2.2. The bound state from  $\Xi_c'\bar{K}$  interaction also appears at a value of  $\alpha$  of about 0.5. To reach the experimental mass of state  $\Omega(3065)$  or  $\Omega(3050)$ , an  $\alpha$  value about 1.0 or 1.5 is required for isoscalar state  $\Xi_c'\bar{K}$  with  $1/2^-$ , respectively.

In Fig. 3, isovector bound states from the interactions  $\Xi_c^{(*)}\bar{K}^{(*)}$  are listed. Generally, one can find that larger  $\alpha$  is required to form an isovector bound state than isoscalar states. It is mainly due to the different flavor signs for the  $\rho$  meson exchange in Table V, which means attraction and repulsion for isoscalar and isovector interaction, respectively.

For three interactions with the  $\bar{K}^*$  meson,  $\Xi_c^*\bar{K}^*$ ,  $\Xi_c'\bar{K}^*$ , or  $\Xi_c\bar{K}^*$ , two bound states with spin parities  $1/2^-$  and  $3/2^-$  appear at an  $\alpha$  value of about 2, which is much larger than

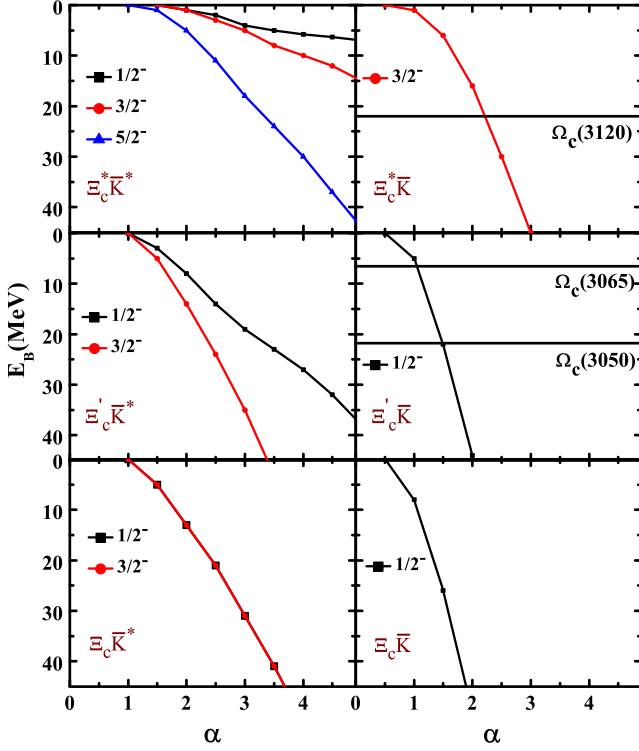


FIG. 2: Binding energies of isoscalar bound states from the interactions  $\Xi_c^{(*)} \bar{K}^{(*)}$  with the variation of  $\alpha$  with single-channel calculation. The horizontal lines are for the experimental values of the masses of corresponding states [28]. The very small uncertainties of masses, only a few tenths of MeV, are not plotted.

these for isoscalar states. The binding energy of the state with spin parity  $3/2^-$  becomes smaller than the states with  $1/2^-$  from interactions  $\Xi_c^* \bar{K}^*$  and  $\Xi_c' \bar{K}^*$ . The isovector  $\Xi_c^* \bar{K}^*$  state with  $5/2^-$  is attractive but too weak to produce a bound state in the considered range of parameter  $\alpha$ . Two  $\Xi_c \bar{K}^*$  states with spin parities  $1/2^-$  and  $3/2^-$  are also almost degenerate as in the isoscalar case.

For three interactions with a  $\bar{K}$  meson involved, only one bound state can be produced as in isoscalar cases. The state with spin parity  $3/2^-$  from interaction  $\Xi_c^* \bar{K}$  appears at a value of  $\alpha$  of about 2 and reaches a binding energy of about 16 MeV at the largest  $\alpha$  value we considered. Compared with the experimental mass of the  $\Omega_c(3120)$ , too large  $\alpha$  of an value is required to assign the isovector  $\Xi_c^* \bar{K}$  state with  $3/2^-$  as  $\Omega_c(3120)$ . For the isovector state  $\Xi_c' \bar{K}$  with spin parity  $1/2^-$ , a binding energy of about 7 MeV can be reached at  $\alpha$  of about 2.2, which is close to mass of the states  $\Omega_c(3065)$  and  $\Omega_c(3050)$ .

#### IV. RESULTS WITH COUPLED-CHANNEL CALCULATION

In the previous section, many bound states are found to be produced from the considered interactions with single-channel calculation in reasonable range of  $\alpha$ . In this section,

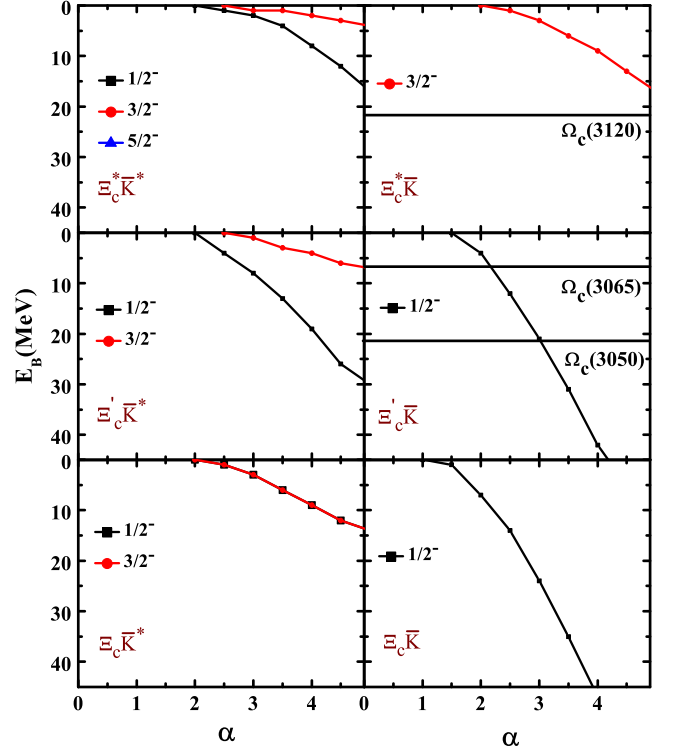


FIG. 3: The binding energies of isovector bound states from the interaction  $\Xi_c^{(*)} \bar{K}^{(*)}$  with the variation of  $\alpha$  with single-channel calculation. The horizontal lines are for the experimental values of the masses of corresponding states [28].

the coupled-channel effects will be introduced to study the variation of the bound states obtained in the previous section and couplings of the molecular states to relevant channels.

##### A. Coupled-channel results for category I

In Table VI, coupled-channel results with all four channels are listed in the third column with the label “cc”. Since the poles are found near the corresponding thresholds, we still present position as  $M_{th} - z$  with  $M_{th}$  being the corresponding threshold as in the single-channel case in the previous section for comparison. Besides, in the fourth to seventh columns, the results for couplings to the channels as labeled are presented with two-channel calculations. The column without an imaginary part is the single-channel results for reference. The couplings of channels above thresholds cannot produce width as expected, which is reflected by a zero imaginary part “0i”.

For isoscalar  $\Xi^* D^*$  states with spin parities  $1/2^-$  and  $3/2^-$ , the introduction of three coupled channels leads to a smaller mass as well as a nonzero width. The pole for the  $\Xi^* D^*$  state with  $1/2^-$  gradually becomes too dim to be seen in the complex plane with the increase of  $\alpha$ . After inclusion of coupled-channel effects, the isoscalar  $\Xi^* D^*$  state with  $5/2^-$  becomes shallower than that with  $3/2^-$ , and its total decay width first increases and then decreases. According to the

TABLE VI: The masses and widths of molecular states from interactions in category I at different values of  $\alpha$  in the unit of GeV. The values of the complex position mean the mass of the corresponding threshold subtracted by the position of a pole,  $M_{th} - z$ , in the unit of MeV. The imaginary part of some poles is shown as 0.0, which means too small a value under the current precision chosen. The explicit explanation can be found in the text.

Poles near the $\Xi^*D^*$ threshold with $M_{th} = 3541.8$ MeV						
$IJ^P$	$\alpha$	$cc$	$\Xi^*D^*$	$\Xi^*D$	$\Xi D^*$	$\Xi D$
$0\frac{1}{2}^-$	1.5	3 + 1.1i	3	4 + 1.7i	4 + 0.2i	4 + 0.0i
	2.0	11 + 1.9i	8	13 + 1.5i	10 + 0.4i	9 + 0.1i
	2.5	19 + 5.1i	14	24 + 2.4i	16 + 0.8i	14 + 0.8i
	3.0	--	19	36 + 3.1i	23 + 0.9i	20 + 2.9i
$0\frac{3}{2}^-$	1.5	4 + 0.0i	4	5 + 0.1i	5 + 0.1i	5 + 0.0i
	2.0	14 + 1.0i	12	12 + 0.2i	14 + 0.7i	13 + 0.1i
	2.5	26 + 2.7i	22	23 + 0.4i	25 + 1.9i	23 + 0.3i
	3.0	41 + 3.5i	34	36 + 1.0i	38 + 3.1i	35 + 0.7i
$0\frac{5}{2}^-$	1.5	5 + 0.8i	5	5 + 0.8i	6 + 0.0i	6 + 0.0i
	2.0	11 + 2.3i	14	11 + 1.5i	15 + 0.1i	14 + 0.2i
	2.5	22 + 1.6i	25	22 + 1.0i	26 + 0.3i	26 + 0.8i
	3.0	37 + 1.7i	40	38 + 0.6i	41 + 0.4i	41 + 1.5i
Poles near the $\Xi^*D$ thresholds with $M_{th} = 3400.6$ MeV						
$IJ^P$	$\alpha$	$cc$	$\Xi^*D^*$	$\Xi^*D$	$\Xi D^*$	$\Xi D$
$0\frac{3}{2}^-$	1.5	4 + 0.7i	4 + 0i	3	4 + 0.6i	3 + 0.0i
	2.0	10 + 1.1i	9 + 0i	8	9 + 1.1i	8 + 0.0i
	2.5	18 + 1.4i	16 + 0i	13	15 + 1.4i	13 + 0.0i
	3.0	30 + 1.5i	26 + 0i	18	22 + 1.5i	18 + 0.1i

imaginary parts in the last three columns, isoscalar state  $\Xi^*D^*$  with  $1/2^-$  has the strongest coupling to the  $\Xi^*D$  channel, while state with  $3/2^-$  state prefers the  $\Xi D^*$  channel. For the  $\Xi^*D^*$  state with  $5/2^-$ , the dominant channel shifts from  $\Xi^*D$  to  $\Xi D$  with the increase of  $\alpha$ . For  $\Xi^*D$  interaction, from which only one state can be formed in the  $S$ -wave with  $3/2^-$ , the coupled-channel effect obviously elevates its binding energy. It can hardly couple to the  $\Xi D$  channel but strongly couple to the  $\Xi D^*$  channel.

### B. Coupled-channel results for category II

In single-channel calculation, the bound states from the interactions in category II are presented, and their relations to the experimentally observed states  $\Omega_c(3120)$ ,  $\Omega_c(3065)$ , and  $\Omega_c(3050)$  are also discussed. In the following, the coupled-channel effects will be investigated. In the single-channel calculation, the  $\Omega_c^{(*)}(\pi/\eta/\rho/\omega)$  interactions are not included due to the absence of exchange of light mesons. Such interactions should be included in the following coupled-channel calculation due to the existence of  $K$  or  $K^*$  exchange between these interactions.

- Poles near the  $\Xi_c^* \bar{K}$  threshold

In the first part of Table VII, we present the coupled-channel results near the  $\Xi_c^* \bar{K}$  threshold, which is close to the state  $\Omega_c(3120)$ . Here, as well as for other thresholds in the table, the couplings to the channels with very high masses are extremely weak. Hence, though the overall coupled-channel results with all ten channels are listed in the “ $cc$ ” column, only four important two-channel results are listed in the table.

TABLE VII: The masses and widths of molecular states from interactions in category II near thresholds with a  $\bar{K}$  meson at different values of  $\alpha$  in the unit of GeV. Other notations are the same as Table VI.

Poles near the $\Xi_c^* \bar{K}$ threshold with $M_{th} = 3142.0$ MeV							
$IJ^P$	$\alpha$	$cc$	$\Omega_c^* \eta$	$\Omega_c \eta$	$\Xi_c^* \bar{K}$	$\Xi_c' \bar{K}$	$\Xi_c \bar{K}$
$0\frac{3}{2}^-$	1.0	1 + 0.0i	1 + 0i	1 + 0i	1	1 + 0.00i	1 + 0.00i
	1.5	8 + 0.02i	8 + 0i	6 + 0i	6	6 + 0.00i	6 + 0.01i
	2.0	21 + 0.05i	20 + 0i	16 + 0i	16	16 + 0.00i	16 + 0.02i
	2.5	40 + 0.12i	36 + 0i	30 + 0i	30	30 + 0.00i	30 + 0.03i
$IJ^P$	$\alpha$	$cc$	$\Xi_c^* \bar{K}$	$\Xi_c' \bar{K}$	$\Xi_c \bar{K}$	$\Omega_c^* \pi$	$\Omega_c \pi$
$1\frac{3}{2}^-$	2.0	1 + 0.4i	0	0 + 0.0i	0 + 0.0i	1 + 0.3i	0 + 0.0i
	2.5	2 + 2.0i	1	1 + 0.0i	1 + 0.0i	2 + 1.5i	1 + 0.0i
	3.0	6 + 4.1i	3	3 + 0.0i	3 + 0.0i	5 + 3.6i	3 + 0.0i
	3.5	13 + 6.6i	6	6 + 0.0i	6 + 0.0i	9 + 4.5i	6 + 0.0i
Poles near the $\Xi_c' \bar{K}$ threshold $M_{th} = 3072.5$ MeV							
$IJ^P$	$\alpha$	$cc$	$\Omega_c^* \eta$	$\Omega_c \eta$	$\Xi_c^* \bar{K}$	$\Xi_c' \bar{K}$	$\Xi_c \bar{K}$
$0\frac{1}{2}^-$	0.7	2 + 0.0i	0 + 0i	0 + 0i	1 + 0i	0	0 + 0.0i
	1.0	13 + 0.0i	5 + 0i	7 + 0i	10 + 0i	5	5 + 0.0i
	1.5	41 + 0.0i	22 + 0i	26 + 0i	34 + 0i	22	22 + 0.0i
	2.0	76 + 0.0i	44 + 0i	50 + 0i	64 + 0i	44	44 + 0.0i
$IJ^P$	$\alpha$	$cc$	$\Xi_c^* \bar{K}$	$\Xi_c' \bar{K}$	$\Xi_c \bar{K}$	$\Omega_c^* \pi$	$\Omega_c \pi$
$1\frac{1}{2}^-$	1.5	4 + 3.8i	2 + 0i	0	0 + 0.0i	0 + 0.0i	0 + 0.0i
	2.0	16 + 9.0i	11 + 0i	4	4 + 0.0i	4 + 0.7i	6 + 5.7i
	2.5	36 + 14.1i	24 + 0i	12	12 + 0.0i	12 + 1.2i	16 + 8.3i
	3.0	62 + 20.3i	39 + 0i	21	21 + 0.0i	22 + 1.8i	29 + 12.2i
Poles near the $\Xi_c \bar{K}$ threshold with $M_{th} = 2965.1$ MeV							
$IJ^P$	$\alpha$	$cc$	$\Omega_c^* \eta$	$\Omega_c \eta$	$\Xi_c^* \bar{K}$	$\Xi_c' \bar{K}$	$\Xi_c \bar{K}$
$0\frac{1}{2}^-$	0.5	0 + 0.0i	0 + 0i	0 + 0i	0 + 0i	0 + 0i	0
	1.0	8 + 0.0i	8 + 0i	8 + 0i	8 + 0i	8 + 0i	8
	1.5	26 + 0.0i	26 + 0i	26 + 0i	26 + 0i	26 + 0i	26
	2.0	50 + 0.0i	50 + 0i	50 + 0i	50 + 0i	50 + 0i	50
$IJ^P$	$\alpha$	$cc$	$\Xi_c^* \bar{K}$	$\Xi_c' \bar{K}$	$\Xi_c \bar{K}$	$\Omega_c^* \pi$	$\Omega_c \pi$
$1\frac{1}{2}^-$	1.5	1 + 0.0i	1 + 0i	1 + 0i	1	1 + 0.0i	1 + 0.0i
	2.0	7 + 0.0i	7 + 0i	7 + 0i	7	7 + 0.0i	7 + 0.0i
	2.5	14 + 0.0i	14 + 0i	14 + 0i	14	14 + 0.0i	14 + 0.0i
	3.0	24 + 0.0i	24 + 0i	24 + 0i	24	24 + 0.0i	24 + 0.0i

According to two-channel calculations, the pole of isoscalar state with spin parity  $3/2^-$  near the  $\Xi_c^* \bar{K}$  threshold is almost motionless after inclusion of channels below the threshold,

$\Xi'_c \bar{K}$ ,  $\Xi_c \bar{K}$ , and the channels above the threshold,  $\Omega_c \eta$ . After inclusion of all channels, the mass of this state becomes a little larger, which leads to a smaller parameter  $\alpha$ , about 2.0, required to reproduce the experimental mass of the  $\Omega_c(3120)$  than in single-channel calculation. The variation of the mass is mainly from inclusion of the  $\Omega_c^* \eta$  channel. The partial width to the  $\Xi_c \bar{K}$  channel is small. If a higher precision is adopted, a value of 0.06 MeV can be found at an  $\alpha$  of 2.5, which is the main decay channel based on the current results. The total width with all channels considered is about 0.2 MeV. If we vary  $\alpha$  to 3, even a width with all channels of about 1 MeV can be reached, which is close to the central value of the experimental value as  $\Gamma_{\Omega_c(3120)} = 1.1 \pm 0.8 \pm 0.4$  MeV.

The results for the isovector  $\Xi_c^* \bar{K}$  state with  $3/2^-$  are also presented in Table VII. In this case, the  $\Omega_c^* \eta$  and  $\Omega_c \eta$  channels are replaced by  $\Omega_c^* \pi$  and  $\Omega_c \pi$  channels, which are both under the threshold. The  $\Omega_c^* \pi$  channel is the dominant decay channel, which gives a width at an order of magnitude of MeV.

- *Poles near the  $\Xi'_c \bar{K}$  threshold*

In the second part of Table VII, we present the results for the states near the  $\Xi'_c \bar{K}$  threshold, which is close to the states  $\Omega_c(3065)$  and  $\Omega_c(3050)$ . For the isoscalar state with  $1/2^-$ , the couplings of channels  $\Omega_c \eta$  and  $\Xi'_c \bar{K}$  make the pole deviate further from the threshold. The partial width to the  $\Xi_c \bar{K}$  channel is much smaller than 0.01 MeV. The mass of the isovector state  $\Xi'_c \bar{K}$  state with  $1/2^-$  is strongly varied by inclusion of the  $\Xi_c^* \bar{K}$  or  $\Omega_c \pi$  channel. And a considerably large width was mainly provided by the coupling to the  $\Omega_c \pi$  channel. Again, a very small partial width to the  $\Xi_c \bar{K}$  channel is found as in the isoscalar case.

- *Poles near the  $\Xi_c \bar{K}$  threshold*

In the last part of Table VII, the poles near the  $\Xi_c \bar{K}$  threshold are presented. For the isoscalar state with  $1/2^-$ , the position of the pole is motionless even after inclusion of all ten channels. Since the  $\Xi_c \bar{K}$  threshold is the lowest one among five channels, the width is zero if no other lower channels are included. The same situation can be found in the isoscalar case, though there exists two channels  $\Omega_c^* \pi$  and  $\Omega_c \pi$  below the thresholds.

- *Poles near the  $\Xi_c^* \bar{K}^*$  threshold*

In Table VIII, the poles near the  $\Xi_c^* \bar{K}^*$  threshold are presented. In the calculation, ten channels are involved, which provide nonzero width. Besides acquiring a width of several MeV, the isoscalar state with spin parity  $1/2^-$  becomes very shallow, and even disappears when the  $\alpha$  increases to about 3.0 due to the repulsive coupled-channel effect in ten-channel calculation. The strongest couplings can be found in the  $\Xi'_c \bar{K}$  channel, and considerable coupled-channel effects are also found in channels  $\Xi_c^* \bar{K}^*$  and  $\Xi_c^* \bar{K}$ . The isoscalar state with  $3/2^-$  becomes a little tight after inclusion of the coupled-channel effect, and a width of about 15 MeV can be acquired with a mass gap about 7 MeV to the threshold at an  $\alpha$  value of 3. The two-channel calculations suggest that the largest coupled-channel effect is from the  $\Omega_c^* \eta$  channel, and channels  $\Xi'_c \bar{K}^*$ ,  $\Xi_c \bar{K}^*$ , and  $\Omega_c \eta$  also provide considerable contributions. For the isoscalar state with  $5/2^-$ , a large width about 40 MeV can be reached at an  $\alpha$  value of about 3. No obvious dominant

channel can be found in the two-channel calculations, and four channels  $\Omega_c^* \eta$ ,  $\Omega_c \eta$ ,  $\Xi_c^* \bar{K}$ , and  $\Xi'_c \bar{K}$  show their strong couplings to this state.

In the isovector sector, there exist two poles with spin parities  $1/2^-$  and  $3/2^-$ . For the state with  $1/2^-$ , the most dominant channel is found in the  $\Xi'_c \bar{K}$  channel. However, the variation of the mass is mainly from the inclusion of the  $\Omega_c^* \rho$  channel. For the state with  $3/2^-$ , the  $\Omega_c^* \pi$  channel provides a large width while the variation of mass is also mainly from the  $\Omega_c^* \rho$  as the case with  $1/2^-$ .

- *Poles near the  $\Xi_c^* \bar{K}^*$  threshold*

In the second part of Table VIII, the results for four poles near the  $\Xi_c^* \bar{K}^*$  threshold are listed. In the isoscalar case, the states with spin parity  $1/2^-$  from the single-channel calculation deviate further from the threshold and acquire a nonzero width. However, with the increase of the  $\alpha$  value, the pole becomes dim in the complex plane. The couplings of the state to the channels  $\Omega_c^* \omega$  and  $\Omega_c^* \eta$  are very weak. All other channels have considerable impact on the mass or width of the state. For the state with  $3/2^-$ , the  $\Xi_c^* \bar{K}$  channel plays an important role in the variation of the mass, while nonzero width is mainly provided by the  $\Omega_c \eta$  channel.

For the isovector state with  $1/2^-$ , the total width is much larger than the sum of the partial widths from the two-channel calculations. It should be from the couplings between the channels besides these involved in the two-channel calculation. For the state with spin parity  $3/2^-$ , the variation of the mass is mainly from the  $\Xi_c^* \bar{K}^*$  channel, and the  $\Omega_c \pi$  channel provides the most important contribution to the total width.

- *Poles near the  $\Xi_c \bar{K}^*$  threshold*

The results for the pole near the  $\Xi_c \bar{K}^*$  threshold are present as the last part of Table VIII. In the single-channel calculation, the  $\Xi_c \bar{K}^*$  states with different  $J^P$  are almost degenerate. After including the coupled-channel effect, the degeneration disappears for all four states. For example, the mass gap between two isoscalar states reaches 5 MeV at an  $\alpha$  value of 3. The differences of the widths of isoscalar and isovector states are also obvious.

In the isoscalar sector, the state with  $1/2^-$  becomes more shallow after including the coupled-channel effect, which is mainly from the couplings to the  $\Xi'_c \bar{K}$  channel. A width about 10 MeV can be reached at  $\alpha$  value of 2, which is mainly from the contribution of the  $\Xi_c \bar{K}$  channel. For the state with  $3/2^-$ , the  $\Xi_c^* \bar{K}$  channel is dominant to produce its total width. And the  $\Xi'_c \bar{K}$  channel also couples to the state strongly.

In the isovector case, the mass of state with  $1/2^-$  decreases obviously after including all channels. However, none of two-channel calculations exhibits such behavior. It should be from the couplings of the channels except the  $\Xi_c \bar{K}^*$  channel. For the same reason, the total width is also much larger than the sum of widths from two-channel calculations. The couplings to the channels  $\Omega_c^* \pi$  and  $\Omega_c \pi$  are found to be important. The state with  $3/2^-$  is shallow even at an  $\alpha$  value of 3.5. Its total width is smaller than the sum of the partial widths as in the case with  $1/2^-$ .





## V. SUMMARY AND DISCUSSION

The molecular states generated from the meson-baryon channels with quantum numbers  $C = 1$ ,  $S = -2$  under 3.6 GeV are studied in a quasipotential Bethe-Salpeter equation approach. With the help of the light meson exchange model, the single-channel and coupled-channel calculations are performed. Based on the results obtained in the current work, the following conclusions can be reached:

- $\Omega_c(3120)$ : Both isoscalar and isovector states can be produced from the  $\Xi_c^* \bar{K}$  interaction with spin parity  $3/2^-$ . The latter requires larger  $\alpha$  value than the former, which can be produced at an  $\alpha$  value of about 1. The state with  $3/2^-$  has very weak coupling to the  $\Xi_c \bar{K}$  channel, which is the observation channel of the  $\Omega_c(3120)$ . Besides, its width increases very rapidly to about 10 MeV with the increase of the parameter. Hence, the isoscalar  $\Xi_c^* \bar{K}$  state is a better candidate of  $\Omega_c(3120)$ . The theoretical width seems small compared with the experimental value, which may be due to absence of light decay channels. Besides, the small partial width of  $\Xi_c \bar{K}$  channel may be the reason why it is difficult to observe in the experiment considering that a molecular state itself should be more hardly produced than a conventional  $\Omega_c$  state. Generally speaking, the isoscalar  $\Xi_c^* \bar{K}$  state with  $3/2^-$  is a good assignment of the  $\Omega_c(3120)$ . Higher-precision measurement should be helpful to confirm it. Besides, an isovector state is also suggested to be observed in the  $\Omega_c \pi$  channel based on the current calculation.
- $\Omega_c(3050)$  and  $\Omega_c(3065)$ : These two states are close to the  $\Xi_c' \bar{K}$  threshold. Based on the calculations in the current work and literature [4, 15, 22, 25], molecular states can be produced from  $\Xi_c' \bar{K}$  interaction with  $1/2^-$ . However, current calculation suggests extremely weak couplings of these states to the experimental observation channel  $\Xi_c \bar{K}$ . Combined with the rejection of the spin parity  $1/2^-$  suggested in Ref. [28], the observed  $\Omega_c(3050)$  and  $\Omega_c(3065)$  should not be the molecular states from the  $\Xi_c' \bar{K}$  interaction. However, it is suggested to search for an isovector state in the  $\Omega_c \pi$  channel.
- The molecular states with higher mass were predicted in the current works. We suggest the experimental research of such states in the future experiment, especially the followings states. Near the  $\Xi^* D^*$  threshold, it is suggested to search the states with  $I(J^P) = 0(1/2^-)$  and  $0(5/2^-)$  in the  $\Xi^* D$  channel, and the state with  $0(3/2^-)$  in the  $\Xi D^*$  channel. The state near the  $\Xi^* D$  threshold with  $0(3/2^-)$  couples strongly to the  $\Xi D^*$  channel. Near the  $\Xi_c^* \bar{K}$  threshold, the states with  $0(1/2^-)$  and  $1(3/2^-)$  are suggested to be searched in the  $\Xi_c' \bar{K}$  channel, and the state with  $0(3/2^-)$  in the  $\Omega_c^* \eta$  channel. The state near the  $\Xi_c' \bar{K}$  threshold with  $0(1/2^-)$  couples strongly to the  $\Omega_c \eta$  channel while that with  $1(3/2^-)$  decays mainly to the  $\Xi \bar{K}$  channel. The states near the  $\Xi_c \bar{K}^*$  threshold with  $0(1/2^-)$  and  $0(3/2^-)$  can be searched in the  $\Xi_c \bar{K}$  channel.

**Acknowledgement** This project is supported by the National Natural Science Foundation of China (Grants No. 11675228).

- 
- [1] R. Aaij *et al.* [LHCb], “Observation of five new narrow  $\Omega_c^0$  states decaying to  $\Xi_c^+ K^-$ ,” *Phys. Rev. Lett.* **118**, 182001 (2017)
  - [2] J. Yelton *et al.* [Belle], “Observation of Excited  $\Omega_c$  Charmed Baryons in  $e^+e^-$  Collisions,” *Phys. Rev. D* **97**, 051102 (2018)
  - [3] G. Chiladze and A. F. Falk, “Phenomenology of new baryons with charm and strangeness,” *Phys. Rev. D* **56**, R6738-R6741 (1997)
  - [4] V. R. Debastiani, J. M. Dias, W. H. Liang and E. Oset, “Molecular  $\Omega_c$  states generated from coupled meson-baryon channels,” *Phys. Rev. D* **97**, 094035 (2018)
  - [5] J. Nieves, R. Pavao and L. Tolos, “ $\Omega_c$  excited states within a  $SU(6)_{\text{sf}} \times \text{HQSS}$  model,” *Eur. Phys. J. C* **78**, no.2, 114 (2018)
  - [6] G. Montaña, A. Feijoo and À. Ramos, “A meson-baryon molecular interpretation for some  $\Omega_c$  excited states,” *Eur. Phys. J. A* **54**, 64 (2018)
  - [7] R. Chen, A. Hosaka and X. Liu, “Searching for possible  $\Omega_c$ -like molecular states from meson-baryon interaction,” *Phys. Rev. D* **97**, 036016 (2018)
  - [8] W. Wang and R. L. Zhu, “Interpretation of the newly observed  $\Omega_c^0$  resonances,” *Phys. Rev. D* **96**, 014024 (2017)
  - [9] B. Chen and X. Liu, “New  $\Omega_c^0$  baryons discovered by LHCb as the members of  $1P$  and  $2S$  states,” *Phys. Rev. D* **96**, 094015 (2017)
  - [10] S. Q. Luo, B. Chen, X. Liu and T. Matsuki, “Predicting a new resonance as charmed-strange baryonic analog of  $D_{s0}^*(2317)$ ,” *Phys. Rev. D* **103**, 074027 (2021)
  - [11] V. O. Galkin and R. N. Faustov, “Heavy Baryon Spectroscopy,” *Phys. Part. Nucl.* **51**, 661-667 (2020)
  - [12] W. Roberts and M. Pervin, “Heavy baryons in a quark model,” *Int. J. Mod. Phys. A* **23**, 2817-2860 (2008)
  - [13] Z. Shah, K. Thakkar, A. Kumar Rai and P. C. Vinodkumar, “Excited State Mass spectra of Singly Charmed Baryons,” *Eur. Phys. J. A* **52**, 313 (2016)
  - [14] T. Yoshida, E. Hiyama, A. Hosaka, M. Oka and K. Sadato, “Spectrum of heavy baryons in the quark model,” *Phys. Rev. D* **92**, 114029 (2015)
  - [15] M. Karliner and J. L. Rosner, “Very narrow excited  $\Omega_c$  baryons,” *Phys. Rev. D* **95**, 114012 (2017)
  - [16] K. L. Wang, L. Y. Xiao, X. H. Zhong and Q. Zhao, “Understanding the newly observed  $\Omega_c$  states through their decays,” *Phys. Rev. D* **95**, 116010 (2017)
  - [17] S. S. Agaev, K. Azizi and H. Sundu, “Interpretation of the new  $\Omega_c^0$  states via their mass and width,” *Eur. Phys. J. C* **77**, 395 (2017)
  - [18] E. Santopinto, A. Giachino, J. Ferretti, H. García-Tecocoatzí, M. A. Bedolla, R. Bijker and E. Ortiz-Pacheco, “The  $\Omega_c$ -puzzle solved by means of quark model predictions,” *Eur. Phys. J. C* **79**, 1012 (2019)
  - [19] H. C. Kim, M. V. Polyakov and M. Praszalowicz, “Possibility of the existence of charmed exotica,” *Phys. Rev. D* **96**, 014009 (2017)
  - [20] C. S. An and H. Chen, “Observed  $\Omega_c^0$  resonances as pentaquark states,” *Phys. Rev. D* **96**, 034012 (2017)
  - [21] H. Huang, J. Ping and F. Wang, “Investigating the excited  $\Omega_c^0$

- states through  $\Xi_c K$  and  $\Xi'_c K$  decay channels,” Phys. Rev. D **97**, 034027 (2018)
- [22] Z. G. Wang, “Analysis of  $\Omega_c(3000)$ ,  $\Omega_c(3050)$ ,  $\Omega_c(3066)$ ,  $\Omega_c(3090)$  and  $\Omega_c(3119)$  with QCD sum rules,” Eur. Phys. J. C **77**, 325 (2017)
- [23] H. X. Chen, Q. Mao, W. Chen, A. Hosaka, X. Liu and S. L. Zhu, “Decay properties of  $P$ -wave charmed baryons from light-cone QCD sum rules,” Phys. Rev. D **95**, 094008 (2017)
- [24] H. X. Chen, W. Chen, Q. Mao, A. Hosaka, X. Liu and S. L. Zhu, “ $P$ -wave charmed baryons from QCD sum rules,” Phys. Rev. D **91**, 054034 (2015)
- [25] M. Padmanath and N. Mathur, “Quantum Numbers of Recently Discovered  $\Omega_c^0$  Baryons from Lattice QCD,” Phys. Rev. Lett. **119**, 042001 (2017)
- [26] H. Y. Cheng and C. W. Chiang, “Quantum numbers of  $\Omega_c$  states and other charmed baryons,” Phys. Rev. D **95**, 094018 (2017)
- [27] Z. Zhao, D. D. Ye and A. Zhang, “Hadronic decay properties of newly observed  $\Omega_c$  baryons,” Phys. Rev. D **95**, 114024 (2017)
- [28] R. Aaij *et al.* [LHCb], “Observation of excited  $\Omega_c^0$  baryons in  $\Omega_b^- \rightarrow \Xi_c^+ K^- \pi^-$  decays,” Phys. Rev. D **104**, 9 (2021)
- [29] H. Y. Cheng, C. Y. Cheung, G. L. Lin, Y. C. Lin, T. M. Yan and H. L. Yu, “Chiral Lagrangians for radiative decays of heavy hadrons,” Phys. Rev. D **47**, 1030-1042 (1993)
- [30] T. M. Yan, H. Y. Cheng, C. Y. Cheung, G. L. Lin, Y. C. Lin and H. L. Yu, “Heavy quark symmetry and chiral dynamics,” Phys. Rev. D **46**, 1148 (1992) Erratum: [Phys. Rev. D **55**, 5851 (1997)].
- [31] M. B. Wise, “Chiral perturbation theory for hadrons containing a heavy quark,” Phys. Rev. D **45**, 2188 (1992).
- [32] R. Casalbuoni, A. Deandrea, N. Di Bartolomeo, R. Gatto, F. Feruglio and G. Nardulli, “Phenomenology of heavy meson chiral Lagrangians,” Phys. Rept. **281**, 145 (1997)
- [33] Y. R. Liu and M. Oka, “ $\Lambda_c N$  bound states revisited,” Phys. Rev. D **85**, 014015 (2012)
- [34] M. Tanabashi *et al.* [Particle Data Group], “Review of Particle Physics,” Phys. Rev. D **98**, 030001 (2018).
- [35] R. Chen, Z. F. Sun, X. Liu and S. L. Zhu, “Strong LHCb evidence supporting the existence of the hidden-charm molecular pentaquarks,” Phys. Rev. D **100**, 011502 (2019)
- [36] C. Isola, M. Ladisa, G. Nardulli and P. Santorelli, “Charming penguins in  $B \rightarrow K^* \pi, K(\rho, \omega, \phi)$  decays,” Phys. Rev. D **68**, 114001 (2003)
- [37] A. F. Falk and M. E. Luke, “Strong decays of excited heavy mesons in chiral perturbation theory,” Phys. Lett. B **292**, 119 (1992)
- [38] J. J. de Swart, “The Octet model and its Clebsch-Gordan coefficients,” Rev. Mod. Phys. **35**, 916-939 (1963) [erratum: Rev. Mod. Phys. **37**, 326-326 (1965)]
- [39] D. Ronchen, M. Doring, F. Huang, H. Haberzettl, J. Haidenbauer, C. Hanhart, S. Krewald, U. G. Meissner and K. Nakayama, “Coupled-channel dynamics in the reactions  $\pi N \rightarrow \pi N, \eta N, K\Lambda, K\Sigma$ ,” Eur. Phys. J. A **49**, 44 (2013)
- [40] A. Matsuyama, T. Sato and T. S. H. Lee, “Dynamical coupled-channel model of meson production reactions in the nucleon resonance region,” Phys. Rept. **439**, 193-253 (2007)
- [41] G. Janssen, K. Holinde and J. Speth, “ $\pi$  rho correlations in the NN potential,” Phys. Rev. C **54**, 2218-2234 (1996)
- [42] A. Reuber, K. Holinde and J. Speth, “Meson exchange hyperon - nucleon interactions in free scattering and nuclear matter,” Nucl. Phys. A **570**, 543 (1994)
- [43] J. T. Zhu, L. Q. Song and J. He, “ $P_{cs}(4459)$  and other possible molecular states from  $\Xi_c^{(*)} \bar{D}^{(*)}$  and  $\Xi'_c \bar{D}^{(*)}$  interactions,” Phys. Rev. D **103**, 074007 (2021)
- [44] J. T. Zhu, S. Y. Kong, Y. Liu and J. He, “Hidden-bottom molecular states from  $\Sigma_b^{(*)} B^{(*)} - \Lambda_b B^{(*)}$  interaction,” Eur. Phys. J. C **80**, 1016 (2020)
- [45] J. He and D. Y. Chen, “Molecular states from  $\Sigma_c^{(*)} \bar{D}^{(*)} - \Lambda_c \bar{D}^{(*)}$  interaction,” Eur. Phys. J. C **79** 887 (2019)
- [46] J. He, “Study of the  $B\bar{B}^*/D\bar{D}^*$  bound states in a Bethe-Salpeter approach,” Phys. Rev. D **90**, 076008 (2014)
- [47] J. He, “The  $Z_c(3900)$  as a resonance from the  $D\bar{D}^*$  interaction,” Phys. Rev. D **92**, 034004 (2015)
- [48] J. He, D. Y. Chen and X. Liu, “New Structure Around 3250 MeV in the Baryonic B Decay and the  $D_0^*(2400)N$  Molecular Hadron,” Eur. Phys. J. C **72**, 2121 (2012)
- [49] J. He, “Internal structures of the nucleon resonances N(1875) and N(2120),” Phys. Rev. C **91**, 018201 (2015)
- [50] J. He, “Nucleon resonances  $N(1875)$  and  $N(2100)$  as strange partners of LHCb pentaquarks,” Phys. Rev. D **95**, 074031 (2017)